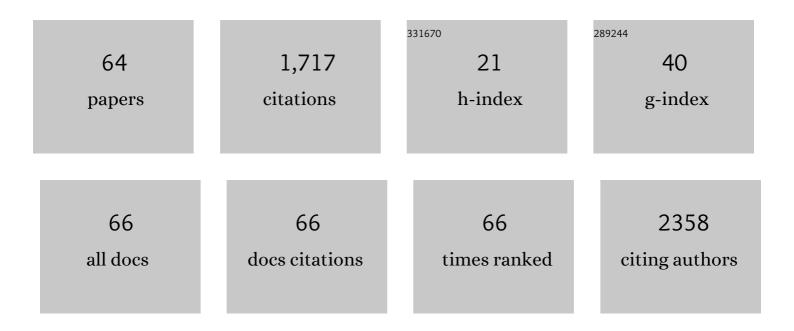
Sungwook Mhin

List of Publications by Year in descending order

Source: https://exaly.com/author-pdf/246679/publications.pdf Version: 2024-02-01



#	Article	IF	CITATIONS
1	Advantageous crystalline–amorphous phase boundary for enhanced electrochemical water oxidation. Energy and Environmental Science, 2019, 12, 2443-2454.	30.8	315
2	Parallelized Reaction Pathway and Stronger Internal Band Bending by Partial Oxidation of Metal Sulfide–Graphene Composites: Important Factors of Synergistic Oxygen Evolution Reaction Enhancement. ACS Catalysis, 2018, 8, 4091-4102.	11.2	116
3	Stable and High-Energy-Density Zn-Ion Rechargeable Batteries Based on a MoS ₂ -Coated Zn Anode. ACS Applied Materials & Interfaces, 2020, 12, 27249-27257.	8.0	110
4	Electrochemically activated cobalt nickel sulfide for an efficient oxygen evolution reaction: partial amorphization and phase control. Journal of Materials Chemistry A, 2019, 7, 3592-3602.	10.3	81
5	Electronically Doubleâ€Layered Metal Boride Hollow Nanoprism as an Excellent and Robust Water Oxidation Electrocatalysts. Advanced Energy Materials, 2019, 9, 1803799.	19.5	74
6	Controllable white upconversion luminescence in Ho3+/Tm3+/Yb3+ co-doped CaMoO4. Journal of Materials Chemistry, 2012, 22, 3997.	6.7	61
7	Graphene Oxide Quantum Dots Derived from Coal for Bioimaging: Facile and Green Approach. Scientific Reports, 2019, 9, 4101.	3.3	57
8	Quasi-intrinsic colossal permittivity in Nb and In co-doped rutile TiO ₂ nanoceramics synthesized through a oxalate chemical-solution route combined with spark plasma sintering. Physical Chemistry Chemical Physics, 2015, 17, 16864-16875.	2.8	51
9	Boosting oxygen evolution reaction of transition metal layered double hydroxide by metalloid incorporation. Nano Energy, 2020, 75, 104945.	16.0	47
10	Ultrafast Method for Selective Design of Graphene Quantum Dots with Highly Efficient Blue Emission. Scientific Reports, 2016, 6, 38423.	3.3	45
11	Dualâ€Phase Engineering of Nickel Borideâ€Hydroxide Nanoparticles toward Highâ€Performance Water Oxidation Electrocatalysts. Advanced Functional Materials, 2020, 30, 2004330.	14.9	44
12	Effect of Fe incorporation on cation distributions and hopping conductions in Ni-Mn-Co-O spinel oxides. Journal of Alloys and Compounds, 2018, 732, 486-490.	5.5	39
13	Sulfur-incorporated nickel-iron layered double hydroxides for effective oxygen evolution reaction in seawater. Applied Surface Science, 2021, 568, 150965.	6.1	34
14	Effect of High Cobalt Concentration on Hopping Motion in Cobalt Manganese Spinel Oxide (Co _{<i>x</i>} Mn _{3–<i>x</i>} O ₄ , <i>x</i> ≥ 2.3). Journal of Physical Chemistry C, 2016, 120, 13667-13674.	3.1	33
15	Stabilizing oxygen intermediates on redox-flexible active sites in multimetallic Ni–Fe–Al–Co layered double hydroxide anodes for excellent alkaline and seawater electrolysis. Journal of Materials Chemistry A, 2021, 9, 27332-27346.	10.3	33
16	A high-performance PDMS-based triboelectric nanogenerator fabricated using surface-modified carbon nanotubes <i>via</i> pulsed laser ablation. Journal of Materials Chemistry A, 2022, 10, 1299-1308.	10.3	32
17	Pulsed Laser Confinement of Single Atomic Catalysts on Carbon Nanotube Matrix for Enhanced Oxygen Evolution Reaction. ACS Nano, 2021, 15, 4416-4428.	14.6	29
18	Few-layered metallic 1T-MoS ₂ /TiO ₂ with exposed (001) facets: two-dimensional nanocomposites for enhanced photocatalytic activities. Physical Chemistry Chemical Physics, 2017, 19, 28207-28215.	2.8	28

SUNGWOOK MHIN

#	Article	IF	CITATIONS
19	Fe doped Ni-Mn-Co-O ceramics with varying Fe content as negative temperature coefficient sensors. Ceramics International, 2017, 43, 10528-10532.	4.8	25
20	Polarized Electronic Configuration in Transition Metal–Fluoride Oxide Hollow Nanoprism for Highly Efficient and Robust Water Splitting. ACS Applied Energy Materials, 2019, 2, 3999-4007.	5.1	24
21	Simple Route for Y[sub 3]Al[sub 5]O[sub 12]:Ce[sup 3+] Colloidal Nanocrystal via Laser Ablation in Deionized Water and its Luminescence. Electrochemical and Solid-State Letters, 2008, 11, J23.	2.2	23
22	Residual neural network-based fully convolutional network for microstructure segmentation. Science and Technology of Welding and Joining, 2020, 25, 282-289.	3.1	23
23	NiFe Layered Double Hydroxide Electrocatalysts for an Efficient Oxygen Evolution Reaction. ACS Applied Energy Materials, 2022, 5, 8592-8600.	5.1	23
24	Simple synthetic route for hydroxyapatite colloidal nanoparticles via a Nd:YAG laser ablation in liquid medium. Applied Physics A: Materials Science and Processing, 2009, 96, 435-440.	2.3	21
25	Phase and texture evolution in solution deposited lead zirconate titanate thin films: Formation and role of the Pt3Pb intermetallic phase. Journal of Applied Physics, 2013, 113, .	2.5	20
26	Luminescence of Nanocrystalline Tb[sub 3]Al[sub 5]O[sub 12]:Ce[sup 3+] Phosphors Synthesized by Nitrate-Citrate Gel Combustion Method. Journal of the Electrochemical Society, 2008, 155, J293.	2.9	19
27	Synthesis of (Ni,Mn,Co)O4 nanopowder with single cubic spinel phase via combustion method. Ceramics International, 2016, 42, 13654-13658.	4.8	18
28	Ni-doped carbon nanotubes fabricated by pulsed laser ablation in liquid as efficient electrocatalysts for oxygen evolution reaction. Applied Surface Science, 2021, 547, 149197.	6.1	17
29	Synthesis of NiCo2O4 Nanostructures and Their Electrochemial Properties for Glucose Detection. Nanomaterials, 2021, 11, 55.	4.1	17
30	Combined Experimental and Computational Methods Reveal the Evolution of Buried Interfaces during Synthesis of Ferroelectric Thin Films. Advanced Materials Interfaces, 2015, 2, 1500181.	3.7	16
31	The effect of pH control on synthesis of Sr doped barium titanate nanopowder by oxalate precipitation method. Ceramics International, 2018, 44, 1420-1424.	4.8	16
32	<i>In situ</i> x-ray diffraction of solution-derived ferroelectric thin films for quantitative phase and texture evolution measurement. Journal of Applied Physics, 2012, 112, .	2.5	14
33	Synthesis of transition metal sulfide and reduced graphene oxide hybrids as efficient electrocatalysts for oxygen evolution reactions. Royal Society Open Science, 2018, 5, 180927.	2.4	14
34	Ti/TiO2/SiO2 multilayer thin films with enhanced spectral selectivity for optical narrow bandpass filters. Scientific Reports, 2022, 12, 32.	3.3	14
35	Oxygen Evolution Reaction of Co-Mn-O Electrocatalyst Prepared by Solution Combustion Synthesis. Catalysts, 2019, 9, 564.	3.5	13
36	Fundamental Understanding of the Formation Mechanism for Graphene Quantum Dots Fabricated by Pulsed Laser Fragmentation in Liquid: Experimental and Theoretical Insight. Small, 2020, 16, 2003538.	10.0	13

SUNGWOOK MHIN

#	Article	IF	CITATIONS
37	Effect of Cu/Fe addition on the microstructures and electrical performances of Ni–Co–Mn oxides. Journal of Alloys and Compounds, 2021, 859, 157769.	5.5	13
38	Niâ€Feâ€Cuâ€layered double hydroxides as highâ€performance electrocatalysts for alkaline water oxidation. International Journal of Energy Research, 2021, 45, 15312-15322.	4.5	13
39	Synthesis of rod-type Co2.4Mn0.6O4 via oxalate precipitation for water splitting catalysts. Applied Surface Science, 2020, 510, 145390.	6.1	12
40	Electrochemical performance of the spinel NiCo2O4 based nanostructure synthesized by chemical bath method for glucose detection. Applied Surface Science, 2021, 545, 148927.	6.1	12
41	Phase evolution of (Ni, Co, Mn)O4 during heat treatment with high temperature in situ X-ray diffraction. Ceramics International, 2016, 42, 5412-5417.	4.8	11
42	Magnetic and magnetotransport properties of Ba2FeMoO6 pulsed laser deposited thin films. Journal of Applied Physics, 2012, 112, .	2.5	9
43	CoFeS2@CoS2 Nanocubes Entangled with CNT for Efficient Bifunctional Performance for Oxygen Evolution and Oxygen Reduction Reactions. Nanomaterials, 2022, 12, 983.	4.1	9
44	Phase and Texture Evolution in Chemically Derived <scp><scp>PZT</scp> </scp> Thin Films on Pt Substrates. Journal of the American Ceramic Society, 2014, 97, 2973-2979.	3.8	8
45	Hopping conduction in (Ni,Co,Mn)O4 prepared by different synthetic routes: Conventional and spark plasma sintering. Ceramics International, 2017, 43, 16070-16075.	4.8	8
46	Facile Design of Conductive Ag-PDMS Electrodes for Stretchable Electrodes. Journal of Electronic Materials, 2019, 48, 79-84.	2.2	8
47	Effect of Switching Atmospheric Conditions during Crystallization on the Phase Evolution of Solutionâ€Derived Lead Zirconate Titanate Thin Films. Journal of the American Ceramic Society, 2013, 96, 2706-2709.	3.8	7
48	Role of the PbTiO 3 Seed Layer on the Crystallization Behavior of PZT Thin Films. Journal of the American Ceramic Society, 2015, 98, 1407-1412.	3.8	7
49	Computational atomicâ€scale design and experimental verification for layered double hydroxide as an efficient alkaline oxygen evolution reaction catalyst. International Journal of Energy Research, 2022, 46, 11972-11988 Synthesis of CoxMn1â~xO4 (0.9 <mml:math (<="")="" 0="" etqq0="" td="" tj="" xmlns:mml="http://www.w3.org/1998/Math/MathML"><td>4.5 0 rgBT /Ov</td><td>6 verloce 10 Tf 5</td></mml:math>	4.5 0 rgBT /Ov	6 verloce 10 Tf 5
50		4.8	5
51	with controlled phase and composition via a gel-combustion method. Ceramics International, 2016, 42, Analysis of structural effect on mechanical stress at backside deep trench isolation using finite element method. Microelectronic Engineering, 2016, 154, 42-47.	2.4	5
52	The effects of oxygen pressure on disordering and magneto-transport properties of Ba2FeMoO6 thin films grown via pulsed laser deposition. Journal of Applied Physics, 2015, 118, 033903.	2.5	4
53	Room Temperature Bonding on Interface Between Metal and Ceramic. Journal of Electronic Materials, 2019, 48, 72-78.	2.2	4
54	Pulsed laser assisted synthesis of Ho3+/Yb3+ codoped CaMoO4 nanocolloid and its upconversion luminescence. Journal of Vacuum Science and Technology B:Nanotechnology and Microelectronics, 2015, 33, .	1.2	3

SUNGWOOK MHIN

#	Article	IF	CITATIONS
55	Crystal structures and electrical properties of cobalt manganese spinel oxides. Materials Today Communications, 2020, 25, 101298.	1.9	3
56	Hierarchical core-shell Ni-Co-Cu-Pd alloys for efficient formic acid oxidation reaction with high mass activity. Applied Surface Science, 2022, 585, 152694.	6.1	3
57	Thermally-driven unequal cation vacancy formation and its effect on the dielectric properties in K0.5Na0.5NbO3 ceramics. Journal of the Korean Physical Society, 2017, 71, 979-985.	0.7	2
58	Roomâ€ŧemperature ferromagnetic organic magnets derived from fluoroâ€graphite via facile halide exchange. International Journal of Applied Ceramic Technology, 0, , .	2.1	1
59	Effect of plasma oxynitriding temperature on wear and corrosion resistance of the AISI 4140 steel. International Journal of Applied Ceramic Technology, 2023, 20, 1002-1009.	2.1	1
60	Crystal Structure of Lu _{2.92} Ce _{0.08} MgAl ₃ SiO ₁₂ Garnet Phosphor and Its Photoluminescent Properties. International Journal of Applied Ceramic Technology, 2016, 13, 228-233.	2.1	0
61	Stress-induced trench narrowing in Cu interconnect of sub-20 nm node: FEM simulation. Materials Science in Semiconductor Processing, 2016, 56, 100-105.	4.0	Ο
62	Graphene Quantum Dots: Fundamental Understanding of the Formation Mechanism for Graphene Quantum Dots Fabricated by Pulsed Laser Fragmentation in Liquid: Experimental and Theoretical Insight (Small 38/2020). Small, 2020, 16, 2070210.	10.0	0
63	Crystal structure of Mn-Co-Ni thermistor. Journal of the Korean Crystal Growth and Crystal Technology, 2015, 25, 225-229.	0.3	Ο
64	Effect of Surface Activated Bonding on Adhesion Strength Between Al and Al2O3. Nanoscience and Nanotechnology Letters, 2017, 9, 1217-1221.	0.4	0